

Experimental report of the proposal

SC 5141 on ID10

1. Scientific background and aim of the project

Phospholipid-porphyrin conjugates (PI-Por) are considered nowadays as the materials of choice for the development of smart drug delivery systems (DDSs) based on their supramolecular assemblies that exhibit multifunctional properties such as photothermal therapy (PTT), photodynamic therapy (PDT)¹⁻³. We have recently synthesized two new series of PI-Por conjugates with different alkyl chain lengths in sn2 position and linked via peptidic bond to either *Pheophorbide-a* (Ph_xLPC , $x = n + 1$, see figure below) or *Pyropheophorbide-a* (Pyr_xLPC , $x = n + 1$) as porphyrin derivatives (Figure 1). Our motivation for changing the length of the alkyl chain in sn2 position is to reduce the chain length mismatch between the two chains. The main aim of the proposed project is to gain insights into the structures and ordering of the pure *PI-Por monolayers and their mixture with other phospholipids (i.e. DPPC) at the air/water interface* by the unique combination of *high energy specular X-ray reflectivity (XRR) and grazing incidence X-ray scattering (GISAXS)*.

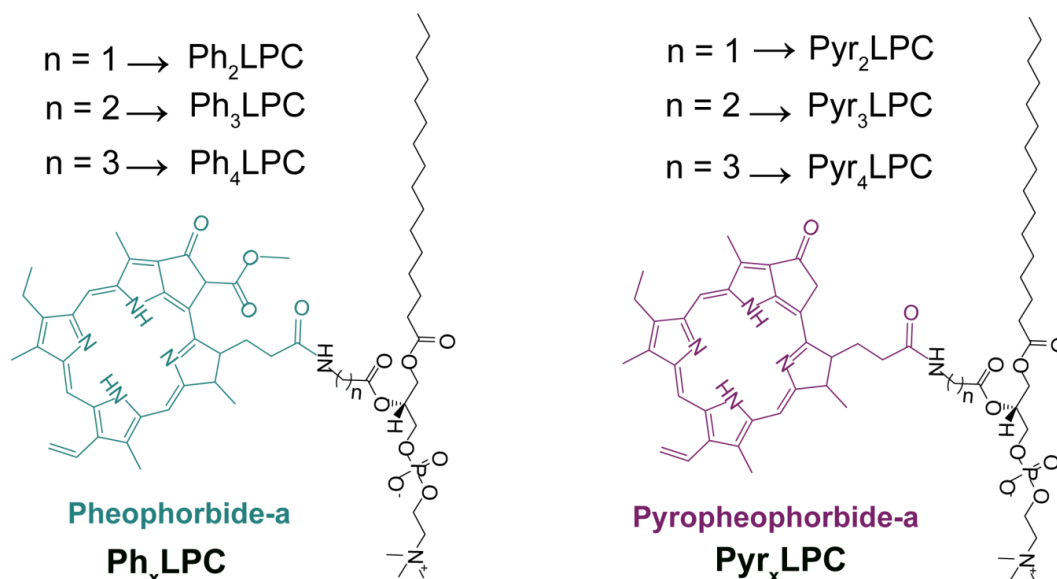


Figure 1: Chemical structures of the studied compounds.

2. Results of experiments

The fine structures of the pure compounds and their mixtures with other phospholipids were determined at different surface pressures. Here we will show the XRR results of the monolayers of pure the compounds at a surface pressure of 30 mN/m.

a. Analysis of the fine structures of Ph_xLPC or Pyr_xLPC monolayers at 30 mN/m probed with XRR

The fine structures perpendicular to the plane of Ph_xLPC and Pyr_xLPC monolayers were studied using XRR. A monolayer of dipalmitoyl phosphatidylcholine (DPPC), a phospholipid with similar polar headgroup (i.e., choline headgroup) and alkyl chain length (16 carbons), was compressed to 30 mN/m and characterized by XRR for the sake of comparison. Figures 2A and 2B, show the XRR curves of DPPC, Ph_xLPC and Pyr_xLPC monolayers, fitted using a two-slab model. The corresponding electron density profiles (ρ) reconstructed from the best fit results (solid black lines in Figures 2A-B) along the z-axis are also shown in Figures 2C-D. The thickness (d), electron density (ρ) and root mean square roughness (σ) of each interface deduced from the best matching fits are summarized in Table 1. For the DPPC monolayer, the calculated total thickness is 24.2 Å, which agrees with literature values for DPPC in the liquid condensed phase. Ph_xLPC monolayers have a total thickness of 16 to 17 Å depending on the spacer length. This 30 % difference in the total thickness of the Ph_xLPC monolayer compared to DPPC is most probably related to the difference in the packing density of the two compounds at 30 mN/m. Indeed, at this surface pressure, Ph_xLPC monolayers display larger molecular areas (57-66 Å²) than DPPC ($A_{30} = 48 \text{ Å}^2$). Thus, Ph_xLPC molecules are less ordered than DPPC ones where the two alkyl chains are aligned in the liquid condensed state. These thickness values are in good agreement with those estimated by AFM. The electron density of the hydrophobic regions of the Ph_xLPC monolayers ($\rho_{\text{HC}} = 0.202\text{-}0.235 \text{ e}^- \cdot \text{Å}^{-3}$) remains almost unchanged compared to DPPC ($\rho_{\text{HC}} = 0.216 \text{ e}^- \cdot \text{Å}^{-3}$) even though Ph_xLPC compounds possess only one alkyl chain per molecule and form more expanded monolayers than DPPC.

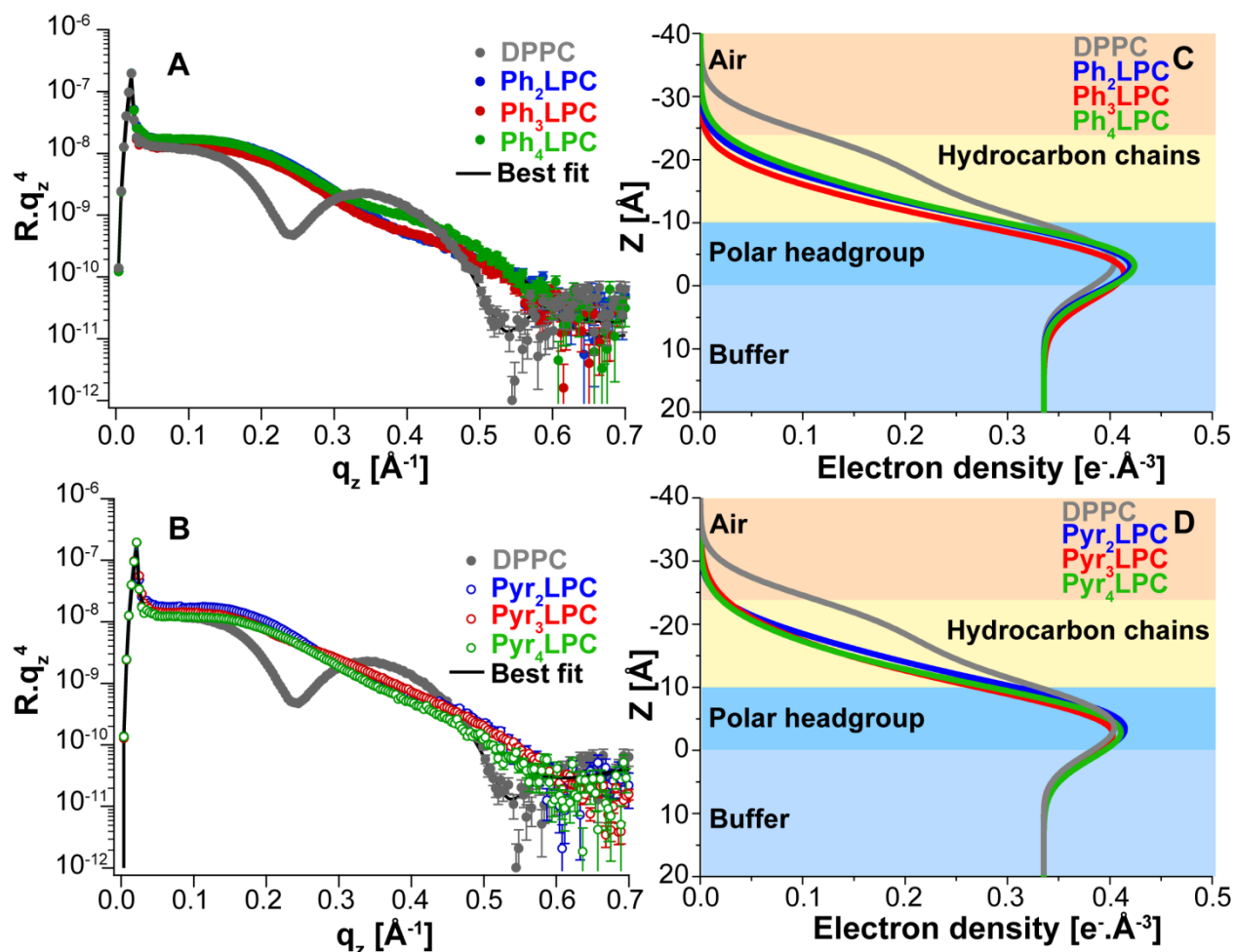


Figure 2: XRR curves of (A) Ph_xLPC and (B) Pyr_xLPC monolayers at a surface pressure of 30 mN/m. The solid lines represent the best model fits to the experimental data. Error bars for the reflectivity data represent the error resulting from the counting statistics. (C) and (D) are the reconstructed electron density profiles (e^- refers to the number of electrons) along the Z-axis for DPPC, Ph_xLPC and Pyr_xLPC compounds.

Conversely, the electron densities of the hydrophilic region ($\rho_{\text{polar}} = 0.475\text{-}0.506 e^- \cdot \text{\AA}^{-3}$) are significantly higher than that of the DPPC choline group ($\rho_{\text{choline}} = 0.418 e^- \cdot \text{\AA}^{-3}$). Given that the total thickness of a Pheo-a monolayer is $\sim 16 \text{\AA}$ at 30 mN/m where the molecules take an upright orientation with respect to the interface, it is plausible that Pheo-a molecules remain at the air/water interface when conjugated to the modified phospholipids. This induces an increase in the electron density in both polar and hydrocarbon regions. Unlike the previously synthesized Ph₆LPC compound ($n = 5$)², the spacer lengths for Ph_xLPC compounds ($n=1, 2$ or 3) are not long enough to allow the porphyrin core to align with the sn-1 C16 carbon chain. This result is in accordance with the isotherm's shape that remains expanded even at high surface pressures. A

similar trend is observed for Pyr_xLPC monolayers, indicating that the latter molecules adopt similar conformations as those of Ph_xLPC. Again, the average thickness of Pyr_xLPC monolayers is consistent with AFM data.

Table 1: Best fit parameters for the XRR Results for DPPC, Ph_xLPC and Pyr_xLPC monolayers at 30 mN/m as presented in Figure 7. The errors are the standard deviations resulting from the Gaussian error propagation during the refinement of the reflectivity curves. (e^- refers to the number of electrons)

	d (Å)	ρ ($e^- \cdot \text{Å}^{-3}$)	σ (Å)
DPPC			
Hydrophobic core	13.6±0.2	0.216±0.025	4.4±0.3
Choline group	10.6±0.4	0.418±0.016	4.4±0.5
Buffer	∞	0.335	3.3±0.2
Ph₂LPC			
Hydrophobic core	8.5±0.2	0.202±0.014	4.8±0.2
Hydrophilic groups	7.5±0.3	0.506±0.014	4.7±0.4
Buffer	∞	0.335	4.1±0.4
Ph₃LPC			
Hydrophobic core	8.6±0.2	0.207±0.011	4.9±0.1
Hydrophilic groups	8.3±0.2	0.481±0.006	4.2±0.1
Buffer	∞	0.335	4.0±0.1
Ph₄LPC			
Hydrophobic core	8.6±0.3	0.235±0.018	5.4±0.2
Hydrophilic groups	8.5±0.5	0.475±0.011	4.0±0.2
Buffer	∞	0.335	3.9±0.3
Pyr₂LPC			
Hydrophobic core	8.2±0.1	0.234±0.014	5.0±0.2
Hydrophilic groups	9.5±0.3	0.449±0.005	3.9±0.1
Buffer	∞	0.335	3.4±0.1
Pyr₃LPC			
Hydrophobic core	8.3±0.4	0.207±0.019	6.1±0.3
Hydrophilic groups	7.9±0.7	0.475±0.019	4.7±0.1
Buffer	∞	0.335	3.7±0.3
Pyr₄LPC			
Hydrophobic core	8.3±0.3	0.198±0.015	5.5±0.3
Hydrophilic groups	8.6±0.3	0.473±0.011	4.5±0.3
Buffer	∞	0.335	4.0±0.2

b. Analysis of the in-plane structure of PI-Por conjugates monolayers

To investigate if the Pyro-a and Pyr_xLPC compounds form crystalline domains at the air/water interface as revealed by AFM data and to determine their size and shape parameters, we studied the in plane structures of the monolayer using GISAXS. The GISAXS data suggests that pure monolayers made of Pyro-a or Pyr_xLPC form crystalline domains at the air/water interface (Figure 3). The domains size and the calculation of the lattice parameter are in progress.

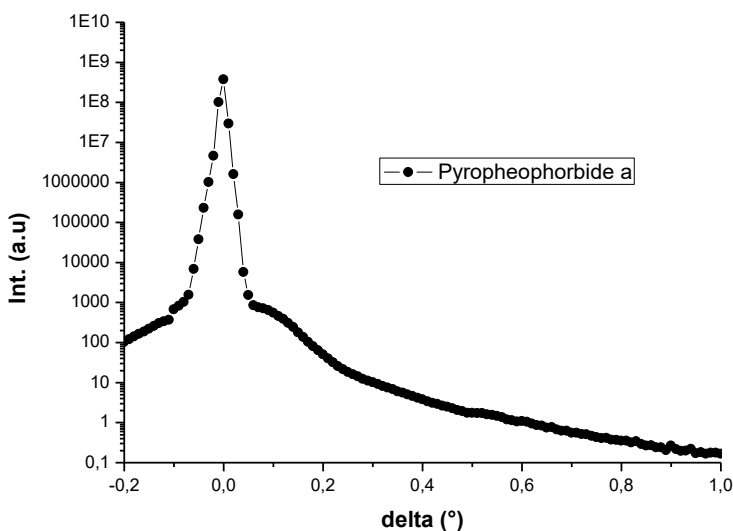


Figure 3: GISAXS signals from Pyropheophorbide-a monolayer at the air/water interface measured at a surface of 30 mN/m.

Summary and Prospects

The allocated beam time allowed us to systematically investigate the fine structures of lipid-porphyrin conjugates monolayers in the absence or presence of other phospholipids such as DPPC. Our XRR data revealed that the PI-Por did not show an alignment between the two chains upon their compression. However the porphyrin core remains at the air/water interface. This would have a great impact on their supramolecular assembly when suspended in aqueous media. These results have been recently published in *Journal of Colloid and Interface Science* (DOI: [10.1016/j.jcis.2021.12.114](https://doi.org/10.1016/j.jcis.2021.12.114)). Further detailed analysis of the GISAXS results are undergoing to get quantitative data on the in-plane structures and will be published soon.

1. J. F. Lovell, C. S. Jin, E. Huynh, H. Jin, C. Kim, J. L. Rubinstein, W. C. Chan, W. Cao, L. V. Wang and G. Zheng, *Nat Mater*, 2011, **10**, 324-332.
2. J. Massiot, V. Rosilio, N. Ibrahim, A. Yamamoto, V. Nicolas, O. Konovalov, M. Tanaka and A. Makky, *Chemistry – A European Journal*, 2018, **24**, 19179-19194.
3. J. Massiot, V. Rosilio and A. Makky, *Journal of Materials Chemistry B*, 2019, **7**, 1805-1823.